

## HRD related signature 3 predicts clinical outcome in advanced tubo-ovarian high-grade serous carcinoma

Heidi Koskela<sup>a,1</sup>, Yilin Li<sup>b,1</sup>, Titta Joutsiniemi<sup>a</sup>, Taru Muranen<sup>b</sup>, Veli-Matti Isoviita<sup>b</sup>, Kaisa Huhtinen<sup>b,c</sup>, Giulia Micoli<sup>b</sup>, Kari Lavikka<sup>b</sup>, Giovanni Marchi<sup>b</sup>, Sakari Hietanen<sup>a</sup>, Anni Virtanen<sup>d</sup>, Sampsa Hautaniemi<sup>b</sup>, Jaana Oikonen<sup>b,\*</sup>, Johanna Hynninen<sup>a,\*</sup>

<sup>a</sup> Department of Obstetrics and Gynecology, University of Turku and Turku University Hospital, Turku, Finland

<sup>b</sup> Research Program in Systems Oncology, Research Programs Unit, Faculty of Medicine, University of Helsinki, Helsinki, Finland

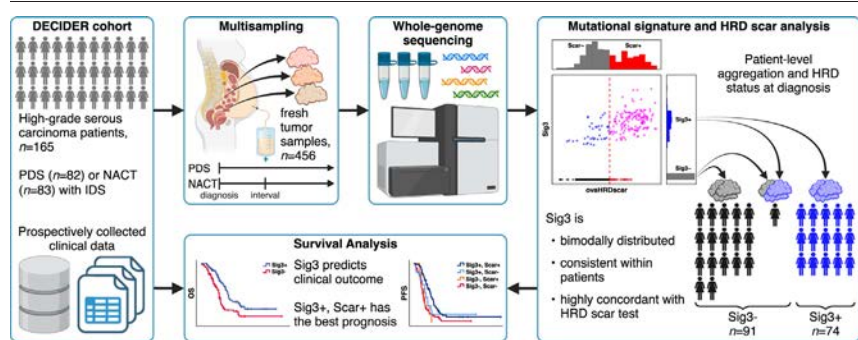
<sup>c</sup> Institute of Biomedicine and FICAN West Cancer Centre, University of Turku and Turku University Hospital, Turku, Finland

<sup>d</sup> Department of Pathology, University of Helsinki and HUS Diagnostic Center, Helsinki University Hospital, Helsinki, Finland

### HIGHLIGHTS

- HRD related single based substitution signature 3 (Sig3) can be used as a prognostic marker for HGSC.
- Sig3 was consistent between multiple samples from the same individuals and status remained after neoadjuvant chemotherapy.
- Sig3 agreed with an HR scar test in 87% of patients, and the worst prognosis was seen in patients without HRD in both tests.

### GRAPHICAL ABSTRACT



### ARTICLE INFO

#### Article history:

Received 13 August 2023

Received in revised form 14 November 2023

Accepted 25 November 2023

Available online xxxx

#### Keywords:

Homologous-recombination-deficiency (HRD)

High-grade serous ovarian cancer (HGSC)

Whole-genome-sequencing (WGS)

Genetic testing

Platinum

### ABSTRACT

**Objectives.** We evaluated usability of single base substitution signature 3 (Sig3) as a biomarker for homologous recombination deficiency (HRD) in tubo-ovarian high-grade serous carcinoma (HGSC).

**Materials and methods.** This prospective observational trial includes 165 patients with advanced HGSC. Fresh tissue samples ( $n = 456$ ) from multiple intra-abdominal areas at diagnosis and after neoadjuvant chemotherapy (NACT) were collected for whole-genome sequencing. Sig3 was assessed by fitting samples independently with COSMIC v3.2 reference signatures. An HR scar assay was applied for comparison. Progression-free survival (PFS) and overall survival (OS) were studied using Kaplan–Meier and Cox regression analysis.

**Results.** Sig3 has a bimodal distribution, eliminating the need for an arbitrary cutoff typical in HR scar tests. Sig3 could be assessed from samples with low (10%) cancer cell proportion and was consistent between multiple samples and stable during NACT. At diagnosis, 74 (45%) patients were HRD (Sig3+), while 91 (55%) were HR proficient (HRP, Sig3-). Sig3+ patients had longer PFS and OS than Sig3- patients (22 vs. 13 months and 51 vs. 34 months respectively, both  $p < 0.001$ ). Sig3 successfully distinguished the poor prognostic HRP group among BRCAwt patients (PFS 19 months for Sig3+ and 13 months for Sig3- patients,  $p < 0.001$ ). However, Sig3 at diagnosis did not predict chemoresponse anymore in the first relapse. The patient-level concordance

\* Corresponding authors.

E-mail address: [mijohy@utu.fi](mailto:mijohy@utu.fi) (J. Hynninen).

<sup>1</sup> Equal contribution.

between Sig3 and HR scar assay was 87%, and patients with HRD according to both tests had the longest median PFS.

**Conclusions.** Sig3 is a prognostic marker in advanced HGSC and useful tool in patient stratification for HRD.  
© 2023 The Authors. Published by Elsevier Inc. This is an open access article under the CC BY license (<http://creativecommons.org/licenses/by/4.0/>).

## 1. Introduction

Tubo-ovarian high-grade serous carcinoma (HGSC) is the most common and aggressive type of ovarian cancer that represents the fifth most common cause of cancer mortality in women [1]. The current first-line treatment for HGSC patients consists of cytoreductive surgery and platinum/taxane-based chemotherapy. In recent years, poly (ADP-ribose) polymerase (PARP) inhibitors have transformed the treatment of ovarian cancer [2,3].

Homologous recombination (HR) has an essential role for maintaining genome stability. HR provides a mechanism for the accurate repair of DNA double-strand breaks and interstrand crosslinks. Homologous recombination deficiency (HRD) is an important therapeutic target as tumor cells with HRD are more susceptible to the DNA cross-linking effect of platinum compounds inducing extensive DNA damage and tumor cell death. PARP proteins are enzymes involved in the DNA repair pathway of single strand breaks. In HR-deficient cells, PARP inhibition induces the simultaneous loss of two critical DNA repair mechanisms, resulting in cell death. Consistently, HGSC patients with HRD have better responses to platinum-based chemotherapy [4] and PARP inhibitors [2,3]. However, accurate identification of HRD status is still a major challenge.

Approximately 50% of HGSCs are HR-deficient [5]. The current ESMO guidelines recommend HRD testing to identify the patients most likely to benefit from a PARPi [6]. HRD testing methodologies are diverse and clinical application remains controversial [6]. Germline deleterious *BRCA1/2* mutations are the best described etiology of HRD [7]. However, HRD can occur due to somatic mutations or epigenetic alterations in *BRCA1/2* or other HR pathway genes. Most commonly used HRD assays today are copy-number-based “scar”-analyses, as there are two prospectively validated commercial tests available and new genomic scar assays are increasingly used and tested for clinical utility [8].

HRD tests that are based on mutational signatures require high-throughput sequencing and computational resources. These signatures reflect the error-prone DNA repair mechanisms employed when HR is compromised, resulting in substitutions, small insertions and deletions (indel), and genomic rearrangements, thus leading to the accumulation of genomic alterations and increased genome instability [9,10]. Specific patterns or mutation types can be decomposed from catalogs of mutations as mutational signatures [11]. Mutational signatures that correlate with prognosis and platinum response in HGSC have been identified [12–14].

Signature 3 (Sig3), also known as SBS3 in COSMIC, is a single base substitution signature. Initially, Sig3 was strongly associated with *BRCA1/2* mutations in breast cancer [15,16]. Furthermore, Sig3 was also found in ovarian and pancreatic cancer [11] and has been proposed as a biomarker for HRD [13]. Sig3-based HRD testing is not in clinical use, and it has been criticized to lack specificity [6]. This is mostly due to the fact that the signature has a uniform-like profile without clear preference to characteristic mutation types.

Herein, we evaluated whether HRD status determined with Sig3 can predict clinical outcome in our prospective cohort of HGSC patients with comprehensive clinical data. We utilized whole-genome sequencing in a multisampling setting to determine the Sig3 status and to compare it to a scar assay. In addition, we evaluated whether Sig3 status at diagnosis predicts response to chemotherapy in disease relapse.

## 2. Methods

### 2.1. Patient characteristics

We collected data from 165 HGSC patients recruited at Turku University Hospital from the DECIDER cohort with FIGO 2014 stages III to IV between 2009 and 2021. DECIDER is a prospective, longitudinal, multi-region observational trial ([clinicaltrials.gov](http://clinicaltrials.gov) ID: NCT04846933) and is approved by the Ethics Committee in the Hospital District of Southwest Finland (ETMK 145/1801/2015). The clinical characteristics of the cohort is described in Table 1.

Patients were treated either with primary debulking surgery (PDS) followed by platinum/taxane-based adjuvant chemotherapy, or with neoadjuvant chemotherapy (NACT) prior to interval debulking surgery (IDS) and adjuvant chemotherapy. A laparoscopic evaluation with diagnostic tumor sampling was performed before NACT. In all, 82 patients were treated with PDS and 83 patients with NACT. Follow-up data were collected until September 2022. The median time of follow-up was 32.9 months, with a range of 1.6 to 153.3 months.

Primary treatment outcome and disease progression were defined with RECIST 1.1 criteria [17]. Progression-free survival (PFS) was defined as the time from diagnosis until first progression. Overall survival (OS) was the time from diagnosis to death. Platinum-free interval (PFI) was calculated from the last dose of platinum-based chemotherapy to first disease progression and was used for patient stratification in second-line treatment analysis. Progression-free survival of second-

**Table 1**  
Clinicopathological characteristics of patients included in the study.

	Sig3+		Sig3-		p-value
	N	%	N	%	
All patients	74	44.8	91	55.2	
Age					<0.001
Median (range) years	65.5		71.0		
	(38.0–83.0)		(52.0–86.0)		
BMI					0.821
Median (range)	26.2		25.9		
	(18.7–39.3)		(17.0–45.3)		
Treatment strategy					0.024
PDS	44	59.5	38	41.8	
NACT	30	40.5	53	58.2	
Stage					0.770
Stage III	48	64.9	61	67.0	
Stage IV	26	35.1	30	33.0	
Residual tumor					0.797
No macroscopic	25	34.7	32	40.0	
<1 cm	35	48.6	36	45.0	
>1 cm	12	16.7	12	15.0	
No data*	2		11		
Number of cycles of chemotherapy					0.019
1–4 cycles	3	4.1	8	8.8	
5–6 cycles	59	79.7	54	59.3	
7–12 cycles	12	16.2	29	31.9	
Bevacizumab maintenance therapy**	37	50.0	37	40.7	0.230

Abbreviations: Sig3, single base substitution signature 3; BMI, body mass index; PDS, primary debulking surgery; NACT, neoadjuvant chemotherapy.

\* Thirteen NACT patients had no interval surgery.

\*\* In the first-line treatment.

line treatment after disease progression (PFSr) was defined as the time from the start of second-line treatment until disease progression or death.

## 2.2. Sample collection and sequencing

We collected 456 fresh tumor samples from multiple intra-abdominal areas at diagnosis ( $n = 385$ ) or after NACT ( $n = 71$ ) for whole-genome sequencing (WGS). Each patient had a matching normal control derived from a blood sample. Sequencing and data processing were performed using Anduril [18] workflows as detailed for the validation cohort in [19] with a tumor cross-sample contamination threshold of 10%. WGS (median 46.9 $\times$  coverage, range 22.3 $\times$ –117.4 $\times$ ) was performed using BGISEQ-500, MGISEQ-2000, or HiSeq X Ten (BGI Europe A/S, Denmark), or NovaSeq 6000 (Novogene (UK) Company Limited, United Kingdom).

We dropped tumor samples with cancer cell proportion (purity) below 10% as estimated by ASCAT [20]. Consequently, we excluded 12.3% of pre-treatment and 49.7% interval samples resulting in the 456 samples. Due to multisampling protocol, we dropped only 3.5% of the patients. Among NACT patients, 65% had interval samples with sufficient purity (38.1% for those with only one interval sample sequenced). Each patient had 1–7 (median 2) treatment-naïve samples, with multiple available for 123 patients. Additionally, 39 patients had 1–8 (median 2) samples from IDS. Most common sampling sites were tubo-ovarian mass ( $n = 134$ ), omentum ( $n = 132$ ), and peritoneum ( $n = 93$ ). Types of samples available in each patient are detailed in Supplementary Table 1.

## 2.3. Signature analysis

COSMIC single base substitution reference signatures v3.2 [21] were corrected for GRCh38 trinucleotide frequencies excluding chromosomes Y and M. Samples were independently fitted with the reference signatures using an R implementation of SigProfilerAttribution [11]. Signatures reported in at least 20% of ovarian cancer samples in COSMIC were selected as starting signatures.

Samples with positive Sig3 contribution were considered HRD. Stratification on ID6, which is an indel signature characterized by microhomology deletions associated with HRD, uses a threshold based on a previously described clustering approach [22]. The ID6 threshold 0.2796 with the optimal F1-score of 0.970 was selected. Samples with ID6 contribution no less than the threshold were considered HRD. Patients with multiple samples were considered HRD only if all the diagnostic samples reported HRD.

As we used three different sequencing platforms, we tested if the sequencing platform influenced HRD prediction. We observed no HRD status discrepancy among samples ( $n = 14$ ) from five patients sequenced with multiple platforms. There was also no significant difference between patients sequenced with a single platform ( $\chi^2$  test,  $p = 0.322$ ) or between samples ( $\chi^2$  test,  $p = 0.390$ ).

## 2.4. Mutation analysis

We curated pathogenic germline variants and somatic driver mutations in the core HR genes, including *BRCA1*, *BRCA2*, *RAD51C*, *RAD51D*, *PALB2*, *BRIP2*, *BARD1*, *ATM*, and *CHEK2*. We considered a genetic change pathogenic, if its consequence in the canonical transcript was premature protein truncation, or if the mutation was annotated pathogenic or likely pathogenic in the ClinVar [23] database. Additionally, the analysis included estimation of loss-of-heterozygosity (LOH) probability and mutation homogeneity in the tumor, integrating mutation allele frequency, the locus copy-number in the tumor samples, and the sample purity. Germline allele frequencies in tumor samples were queried using GATK 4.1.9.0 [24] Mutect2 forced calling.

## 2.5. OvaHRDscar analysis

We estimated HRD scar levels using somatic copy-number alterations from a Nextflow [25] pipeline that integrates structural variants. The structural variants were jointly called using GRIDSS 2.13.2 [26] while segmentation and allele-specific copy-number inference were performed using PURPLE 3.7.2 [27]. We used WGS samples with cross-sample contamination below 3%, and obtained the results from all available samples included in the signature analysis. The scar levels and corresponding HRD classifications were computed using ovaHRDscar [8]. Patient was considered HRD if all samples were HRD, similarly to mutational signatures.

## 2.6. Statistical analysis

Descriptive statistics were used to summarize the clinical characteristics of the study population. Associations were assessed by the  $\chi^2$  test and the Mann–Whitney test. Survival analyses were performed with the Kaplan–Meier method and with multivariable Cox regression analyses, and differences in survival were analyzed with a log-rank test. For all statistical analyses, significant differences were set as  $p < 0.05$ . Statistical analyses were performed using IBM SPSS Statistics 27 (IBM Corp., Armonk, N.Y., USA).

## 3. Results

### 3.1. HRD stratification with Sig3

We stratified patients to HRD and HR proficient (HRP) groups based on Sig3 (Fig. 1). As Sig3 was clearly bimodally distributed without overlap, either zero or within 0.275–0.721 (Fig. 2A), Sig3-positive (Sig3+) samples were considered HRD and no further threshold optimization was needed. Totally, 45% of patients (74/165) had only Sig3+ samples and were considered HRD (Fig. 1).

Though we set the cancer cell proportion (purity) threshold to 10%, we observed that including samples with purity as low as 5%, i.e., minimum amount detectable by ASCAT [20], did not increase the number of patients with discordant HRD status. Similarly, increasing the threshold did not decrease the proportion of discrepant patients.

We compared Sig3 with ID6-based classification, observing 86% concordance among patients and 85% among samples (Fig. 1, 2A). Due to the limited power to analyze indel signatures outside of WGS [28], especially at low purity samples, and a more complex threshold determination of ID6, we focused on Sig3 in subsequent analyses.

### 3.2. Sig3 and mutations within HR pathway in the WGS data

We have previously analyzed the DECIDER cohort ( $n = 131$  patients described herein) for somatic variants and copy-number aberrations, including those affecting HR pathway driver genes [19]. Herein, these gene mutations were expert curated and included germline and structural variants related to HRD. This analysis revealed 31 (19%) patients with 32 loss-of-function mutations accompanied with loss-of-heterozygosity (LOH). The mutations were found in *BRCA1*, *BRCA2*, *RAD51C*, *RAD51D*, and *BRIP1* (Fig. 1, Supplementary Table 2). Notably, no carriers of the Finnish founder mutations in *PALB2*, *CHEK2*, or *ATM* were detected in this patient cohort. These mutations except for *RAD51C*:p.R312Q were protein truncating mutations, 17 originating from patient germline, 15 as somatic events. The most commonly affected gene was *BRCA1*, with five germline carriers and nine patients with somatic mutations. The tumor samples from patients with complete loss of the function of *BRCA1/2* or *RAD51C/D* were all concordantly Sig3+ (29 out of 74 Sig3+ patients). The samples from the two patients with loss of *BRIP1* function in the tumor were Sig3-, but positive for the ID6 signature.

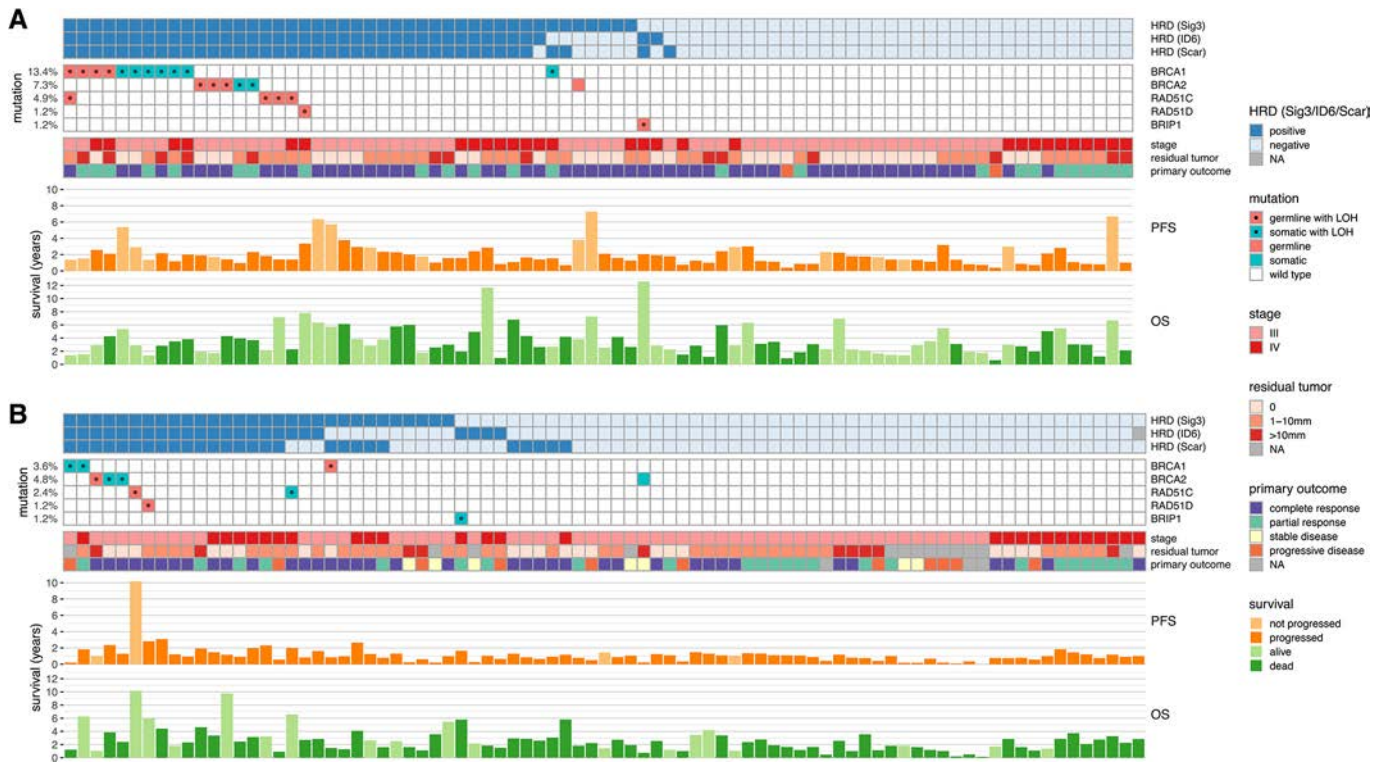


**Fig. 1.** Cohort HR status and clinical data. Patients are stratified by treatment strategy with **A.** PDS in the top panel and **B.** NACT in the bottom panel. Dots on HR gene mutations represent copy-number loss-of-heterozygosity and are only shown when accompanying a mutation, indicating homogeneous biallelic loss of the gene. Gene mutation frequencies on the left include cases without loss-of-heterozygosity. NACT patients with NA for residual tumor did not undergo debulking surgery. Patients whose primary treatment was stopped are considered NA in primary outcome. See Supplementary Fig. 1 for heterogeneity indications. Sig3, single base substitution signature 3; Scar, ovaHRDscar; HRD, homologous recombination deficiency; PFS, progression-free survival; OS, overall survival; LOH, loss-of-heterozygosity; PDS, primary debulking surgery; NACT, neoadjuvant chemotherapy; NA, not available.

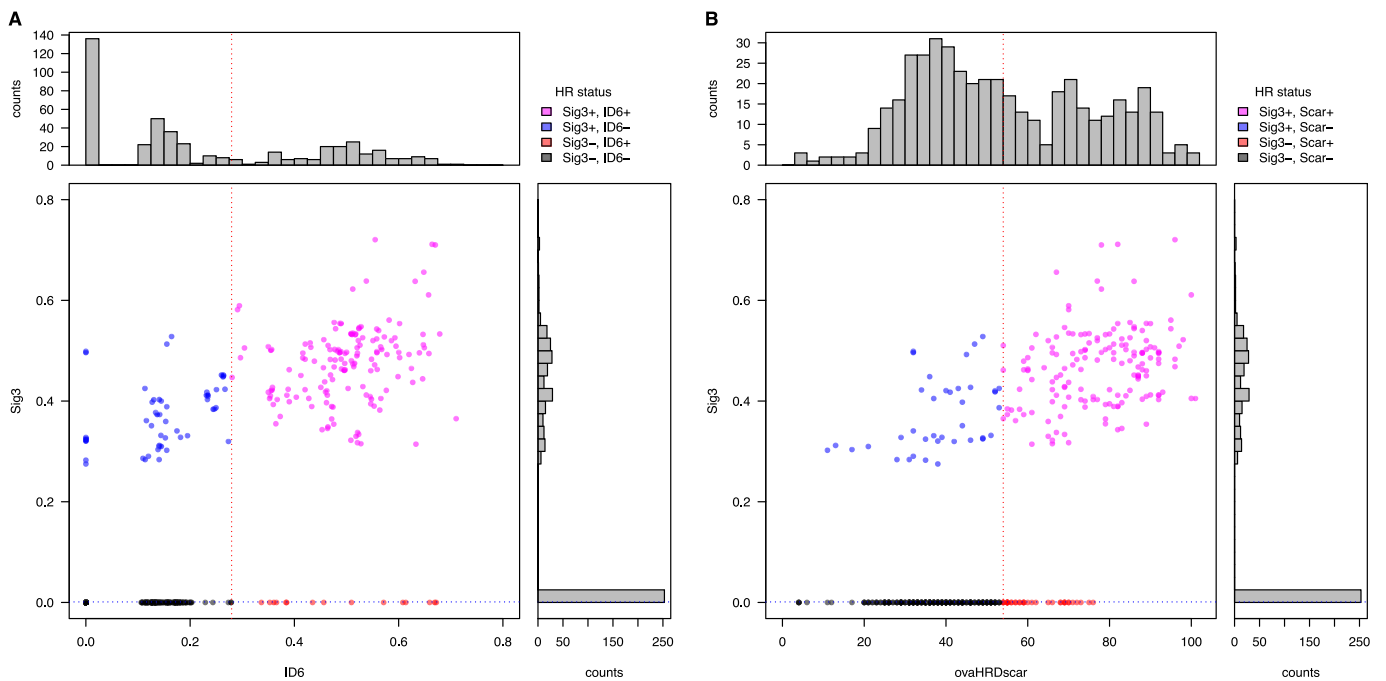


**Fig. 2.** Distribution of sample ID6 contributions and ovaHRDscar levels against Sig3 contributions. Sample Sig3 is compared against **A.** ID6 contribution and **B.** ovaHRDscar levels. All diagnostic and interval samples analyzed in respective quantities are shown in the scatter plots and marginal histograms. The histograms use left-closed intervals. Sig3, single base substitution signature 3; Scar, ovaHRDscar.

### 3.3. Sig3 is consistent between intra-abdominal sampling sites and during NACT

Multi-sampling design of the DECIDER cohort enables quantifying HRD heterogeneity within patients. Sig3 was highly consistent in the majority of 123 patients, with only five (4%) patients having heterogeneous Sig3 at diagnosis. Four of these had tubo-ovarian samples available for analysis. These allegedly primary site samples were all Sig3-positive (Sig3+), while the metastatic intra-peritoneal samples were all the Sig3-negative (Sig3-). This indicates that residual disease after surgery can be HRP and these patients were considered HRP (Supplementary Fig. 1).

Only two patients (5%,  $n = 39$ ) had discordant HRD status between diagnostic and interval samples (Supplementary Fig. 1B). For one patient, Sig3 was likely missed in one interval ascites sample due to its low purity of 11%. For the other patient, the sole adnexal sample, taken during IDS, was Sig3-. The other four pre-treatment and interval samples were Sig3+. The adnexal sample shared only around half of the mutations with the other four samples, indicating HRD being subclonal.

### 3.4. HRP (Sig3-) patients were older and more often scheduled for NACT

HRP patients were significantly older ( $p < 0.001$ , Fig. 3, Table 1) and more often treated with NACT ( $p = 0.024$ ). Younger age of Sig3+ patients at diagnosis were not explained by germline HR gene mutations associated with earlier disease onset. No difference was found in FIGO 2014 stage, patients' body mass index (BMI), residual tumor in surgery, or the number of patients treated with bevacizumab maintenance therapy in the first-line treatment, between the Sig3 groups (Table 1).

### 3.5. Sig3 predicts PFS and OS

At the end of the follow-up period, 62 patients were alive and 103 were dead. PFS and OS were significantly longer in patients with Sig3+ cancer (Fig. 4A and B). The median PFS in Sig3+ group was 22.1 months compared to Sig3- group where it was 12.7 months ( $p < 0.001$ ). Concordantly, the median OS was 50.5 and 33.6 months in Sig3+ and Sig3- groups, respectively ( $p < 0.001$ ). Additionally, primary therapy outcomes differed significantly ( $p = 0.039$ , Table 2). Ten (11.0%) patients with Sig3- cancer but only three (4.1%) patients with Sig3+ cancer had progressive disease during primary therapy.

Negative status for Sig3 predicted worse PFS in the whole cohort (HR 2.36, CI 1.61–3.46,  $p < 0.001$ ) in multivariable Cox regression analysis (Supplementary Table 3). Additionally, patients treated with NACT had worse PFS compared to patients treated with PDS (HR 3.10, CI 2.15–4.50,  $p < 0.001$ ). There was no significant effect of FIGO 2014 stage (stage IV vs. stage III), age at diagnosis, residual tumor (R2 or no debulking surgery vs. R0–R1), bevacizumab treatment, or first-line PARPi treatment.

Sig3+ patients with detected mutation in HR pathway genes *BRCA1/2* or *RAD51C/D* had 5.1 months longer median PFS than Sig3+ patients with wild-type *BRCA/RAD51* (24.2 months vs. 19.1 months, Fig. 4C), but the difference was not statistically significant ( $p = 0.314$ ). Importantly, Sig3+ patients with wild-type *BRCA/RAD51* had significantly longer median PFS than Sig3- patients (19.1 vs. 12.7 months,  $p < 0.001$ ).

### 3.6. Response to second-line chemotherapy depends on PFI, not HRD status

We then evaluated whether Sig3 status at diagnosis predicts response to platinum-based chemotherapy in the second line. A majority, 142 of 155 patients (91.6%) developed recurrent cancer within two years of follow-up. In addition, ten patients without disease progression had a follow-up period of less than two years. Because of a higher proportion of PFI > 6 months in Sig3+ patients (Table 2), they were more often treated with platinum-based chemotherapy at the first progression (48/59, 81.4%) than Sig3- patients (54/82, 65.9%). Median progression-free survival of second-line treatment (PFSr) was only 1.5 months longer in Sig3+ patients and the difference was not statistically significant.

As PFI is a major prognostic factor [28], we performed a subgroup analysis including three subgroups: patients with PFI < 6 months, patients with Sig3+ and PFI > 6 months, and patients with Sig3- and PFI > 6 months. Patients with PFI < 6 months were combined into one subgroup, because they had similar survival despite the Sig3 status: the patients with PFI < 6 months had the shortest median PFSr in the 2nd line ( $p < 0.001$ ). Similarly, there was no statistically significant difference between Sig3+ and Sig3- patients in PFSr in patients with PFI > 6 months (Fig. 4D). In conclusion, Sig3 status had no predictive power on treatment response in the first progression.

### 3.7. Sig3+ patients benefited from PARP inhibitors

During the study period, PARPis were entering clinical use. In total, 40 patients were treated with PARPi therapy: 14 patients as

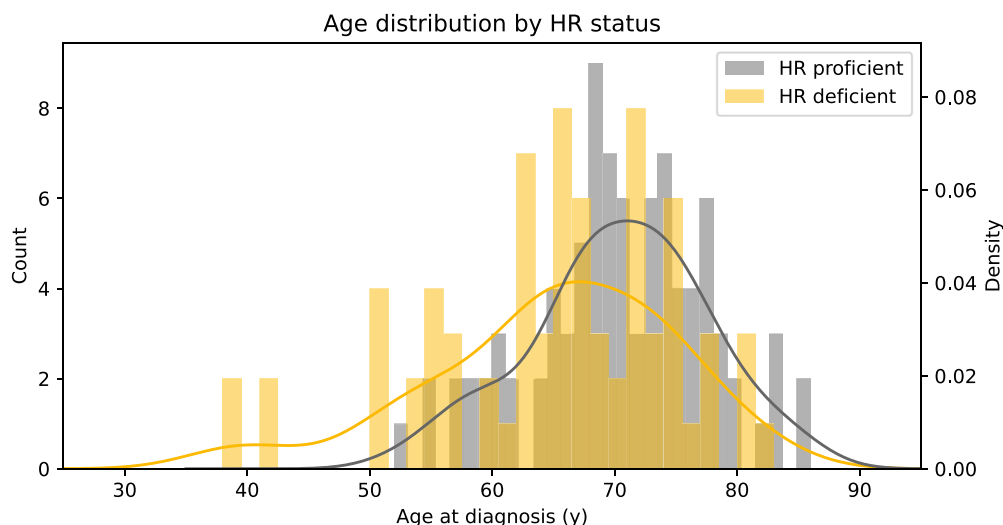
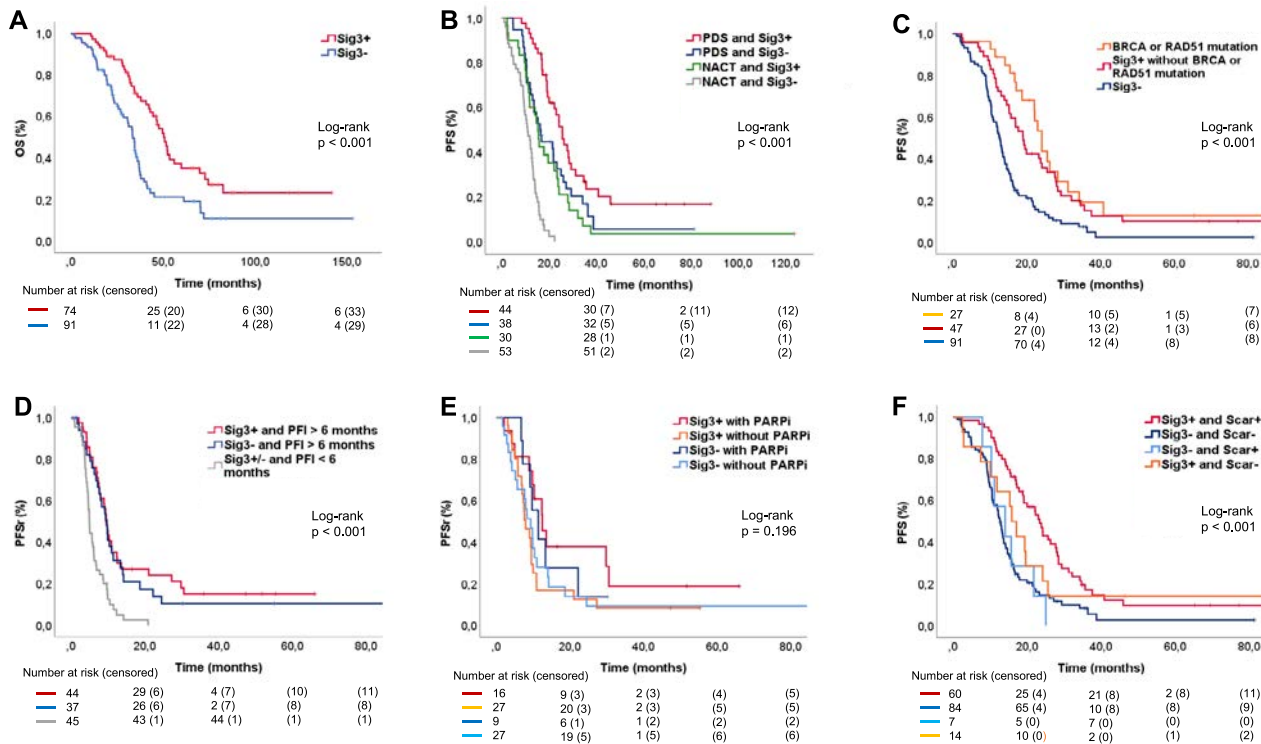


Fig. 3. Distribution of age at diagnosis stratified by HR status. Patients are HR-deficient if all diagnostic samples are Sig3+. HR, homologous recombination.



**Fig. 4.** Kaplan–Meier survival curves of progression-free survival and overall survival. **A.** OS in the whole cohort ( $p < 0.001$ ). **B.** PFS of first-line treatment stratified by treatment strategy. Patients with Sig3+ and treated with PDS had the longest PFS ( $p < 0.001$ ). In all, NACT patients had shorter PFS compared to PDS patients. **C.** PFS of first-line treatment stratified by BRCA1/2 or RAD51C/D mutation status and Sig3. **D.** PFSr of second-line treatment stratified by PFI  $<$  or  $>$  6 months before first disease progression. As patients with PFI  $<$  6 months had similar PFSr despite the Sig3 status, they were combined into one subgroup, and had the shortest PFSr ( $p < 0.001$ ). No statistically significant difference was found in the PFSr in the second line, if a patient had PFI  $>$  6 months. **E.** PFSr of second-line treatment in patients with or without PARPi therapy started in the second line. In survival analysis, all patients had PFI  $>$  6 months. **F.** PFS of first-line treatment jointly stratified by Sig3 and ovaHRDscar. Sixty patients were positive for both tests, 14 and seven only for Sig3 and ovaHRDscar respectively, and 84 were considered HRP by b. OS, overall survival; PFS, progression-free survival; Sig3, single base substitution signature 3; PDS, primary debulking surgery; NACT, neoadjuvant chemotherapy; PFSr, progression-free survival of second-line treatment; PFI, platinum-free interval; PARPi, poly (ADP-ribose) polymerase inhibitor; HRP, homologous recombination proficient.

maintenance in the first line and 27 after first disease progression. A total of 20 patients (74.1%) treated with PARPis after first disease progression had stopped the therapy during the follow-up due to progression or adverse effects. The median duration of treatment was 6.8 months (range 0.7–19.1 months). Seven patients had on-going PARPi treatment at the time the follow-up data was collected.

Sig3+ patients with PFI  $>$  6 months before first progression had 4.6 months longer median PFSr if they were treated with PARPi therapy in the second line ( $p = 0.049$ , Fig. 4E). Also, in the Sig3- group, the median PFSr was 2.1 months longer in patients treated with PARPi therapy but that was not statistically significant ( $p = 0.372$ , Fig. 4E).

**Table 2**  
Responses to first-line treatment.

	Sig3+		Sig3-		p-value
	N	%	N	%	
All patients	74	44.8	91	55.2	
Primary therapy outcome					
Complete response	51	68.9	43	47.3	<b>0.039</b>
Partial response	18	24.3	30	33.0	
Stable disease	2	2.7	5	5.5	
Progressive disease	3	4.1	10	11.0	
Chemotherapy stopped due to side effects			3	3.3	
PFI*					
<6 months	13	21.7	42	51.2	<b>&lt;0.001</b>
6–12 months	12	20.0	26	31.7	
>12 months	35	58.3	14	17.1	

Abbreviations: Sig3, single base substitution signature 3; PFI, platinum-free interval.  
\* PFI of patients ( $n = 142$ ) with first progression.

### 3.8. Combination of Sig3 and HR-scar assay improves PFS prediction

Scar-based HRD-assays are increasingly used in the clinic. We recently published a scar assay optimized for HGSC called ovaHRDscar, featuring an analysis that includes 30 patients from the cohort presented herein [8]. SNP-array-based ovaHRDscar (HUSLAB laboratory) has received clinical approval in Finland and serves as the foundation for the reimbursement of PARP inhibitors. For comparison with Sig3, we now applied ovaHRDscar to the full cohort. With ovaHRDscar, 67 (41%) patients were HRD and 98 (59%) HRP. Concordance between Sig3 and ovaHRDscar was 87% among patients and 84% among samples (Fig. 1, 2B). Furthermore, eleven patients in our cohort were also tested with Myriad MyChoice® CDx which was successful in ten patients. Of these, nine (90%) had concordant results with Sig3, which despite the low sample size was not dissimilar from the concordance of Sig3 with ovaHRDscar.

Next, we focused on patients with heterogeneous ovaHRDscar-statuses. Their scar levels were proximal to the threshold (54), with most having exclusively Sig3- samples (Supplementary Fig. 2). Furthermore, seven Sig3- and ovaHRDscar-positive (Scar+) patients had lower scar levels compared to patients with concordant HRD statuses. Notably, a patient with biallelic loss of RAD51C was HRP due to scar levels being just under the cutoff value. These results likely reflect the spectrum of genomic scarring due to HRD in these patients instead of HRD being a strictly binary trait (Fig. 2B). In all, 60 (36%) patients were HRD and 84 (51%) were HRP with both methods. Twenty-one (13%) patients had discrepant results.

Moreover, we performed survival analysis between Sig3 and ovaHRDscar-based HR status (Fig. 4F). Patients positive for both Sig3 and ovaHRDscar had the longest median PFS (23.4 months). The

median PFS of patients with Sig3- and ovaHRDscar-negative (Scar-) tumors was only 12.7 months ( $p < 0.001$ ). Interestingly, those patients with discrepancy between aforementioned HRD tests, either Sig3-/Scar+ or Sig3+/Scar-, had median PFS notably shorter than patients with both tests positive (14.0 and 15.8 months, respectively).

#### 4. Discussion

New personalized treatments are urgently needed for HGSC patients and WGS is increasingly used to search for druggable genomic alterations. As HRD is a major prognostic factor and predicts PARPi response, HRD status has to be determined before exploring alternative treatment options. HRD-related mutational signature 3 (Sig3) is used in research projects that involve WGS to stratify patients by their HRD status [29], but its clinical usefulness has not been established. Here, we have shown that Sig3 predicts PFS and OS in advanced HGSC and can be assessed from samples with low purity.

Our method to estimate HRD with Sig3 from WGS data was adapted from Alexandrov et al. [11], who extracted >50 distinct mutational signatures in large pan-cancer cohorts without studying prognostic associations. Herein, we report that median PFS and OS were significantly longer in HRD (Sig3+) patients than HRP patients (PFS 22.1 vs. 12.7 months, OS 51 vs. 34 months). Consistently, Sig3+ has been associated with better survival in the Ovarian cancer TCGA WES dataset when estimated with the computational tool SigMA [13], and in a Canadian cancer registry-based study [30].

Our Sig3- patients were more often directed to NACT, but this was not explained by their older age or FIGO stage. The decision to start NACT is based on multiple factors like age, comorbidities and disease spread. It is possible that intra-abdominal spread pattern in HRP patients may favor NACT, and this should be evaluated in future trials.

HRD is typically analyzed in tubo-ovarian primary tumors in the clinic, as are mutational signatures in large studies [11,15,31]. In the current study with up to 123 multisampled patients, we were able to show that HRD variation between anatomical sites is rare. Before treatment, 11% of patients had discrepant scar-based statuses and only 4% in terms of Sig3. In line with our results, Sig3 heterogeneity was infrequent in two small cohorts [32,33]. Sig3 status remained also consistent before and after NACT in 95% of our patients. Taken together, HRD status can be determined with Sig3 from a single sample, irrespective of anatomical site. IDS samples can also be utilized in the absence of diagnostic samples, although multiple samples are needed to address detection challenge caused by small amount of surviving cells. Notably, we were able to define Sig3 from samples with a purity of 10%, while HRD tests typically need 20%–30% tumor content.

Interestingly, Sig3 determined at the time of diagnosis predicted response to first-line platinum treatment in our cohort, but not the second line. Given that response to platinum rechallenge in the first relapse was similar in all patients with PFI > 6 months, they should be offered active treatment regardless of their HRD status. Sig3's limited predictive value for relapse treatment can be explained by the limitation of both mutational signature and scar based HRD analyses as they both rely on historic events. Changes from HRD to HRP cannot be detected, even though novel reversion mutations or promoter demethylation would restore the HR activity in the tumor cells [34]. In the future, timely HR status for disease relapse may be determined with functional HRD testing, such as RAD51 immunostaining [22].

Currently, the most important clinical purpose of the HRD testing is patient selection to PARPi therapy. Existing prospective clinical trials have primarily relied on HR scar tests with varying cutoff values and methodologies for patient stratification. There is a clear need for improved biomarkers, especially in BRCAwt patients, as tests fail to consistently identify a BRCAwt subgroup that derives no benefit from PARPi [3,35]. Studies correlating Sig3 and response to PARPi are sparse, although phase I/II trials [36,37] and a preclinical study [38] have shown

promise. In the present study, Sig3+ patients benefited from PARPi therapy after platinum sensitive relapse. Further studies are needed to evaluate clinical validity of Sig3-based assay for predicting PARPi benefit in HGSC.

Our results indicate that Sig3 offers additional value to HR scar tests. Sig3 successfully distinguished the poor prognostic HRP group among BRCAwt patients. Sig3 exhibited robust and binary signature fits (Fig. 2), eliminating the need for threshold optimization. This finding is important as mutational signature-based HRD assays have faced criticism for the difficulty in determining proper thresholds [6]. In our study, Sig3 and ovaHRDscar exhibited strong agreement, but interestingly the patients classified as HRP with both tests had the shortest median PFS. Evaluating Sig3 in combination with established biomarkers could provide additional insights and enhance predictive accuracy.

The strengths of the current study are prospectively collected clinical data and a meticulous multisampling protocol. Diverse chemotherapy regimens used in relapse treatments and PARPi therapy entering the clinic during study period can be seen as limitations. This reflects the real-life situation where the study is conducted. WGS analyses are considered relatively expensive and time-consuming and thus WGS data are not widely available in clinics. However, turnaround time for WGS can be optimized to <10 days [39], and the cost is comparable to commercial HRD assays [40–42]. Furthermore, sequence data availability is increasing which warrants new methods to widen usability of such data in personalized treatment of HGSC.

In conclusion, our results indicate that WGS-based single base substitution signature 3 can reliably identify cancers with HRD and serves as a prognostic marker in advanced HGSC. Additionally, it can be measured from samples with low cancer cell proportion and from various metastatic sites. When sequencing data is available, patient stratification with Sig3 at diagnosis enables to select patients for further genomic analyses and individual treatment approaches.

Supplementary data to this article can be found online at <https://doi.org/10.1016/j.ygyno.2023.11.027>.

#### Code availability

The code for processing sequencing data including signature analysis is available upon request.

#### CRediT authorship contribution statement

**Heidi Koskela:** Formal analysis, Investigation, Data curation, Writing – original draft, Visualization. **Yilin Li:** Methodology, Software, Formal analysis, Data curation, Writing – original draft, Visualization. **Titta Joutsiniemi:** Investigation, Writing – review & editing. **Taru Muranen:** Formal analysis, Data curation, Writing – original draft. **Veli-Matti Isoviita:** Writing – review & editing, Visualization. **Kaisa Huhtinen:** Investigation, Data curation, Writing – review & editing. **Giulia Micoli:** Software, Formal analysis, Writing – review & editing. **Kari Lavikka:** Software, Formal analysis, Writing – review & editing. **Giovanni Marchi:** Software, Formal analysis, Data curation, Writing – review & editing. **Sakari Hietanen:** Resources, Writing – review & editing. **Anni Virtanen:** Conceptualization, Writing – review & editing. **Sampsa Hautaniemi:** Conceptualization, Writing – review & editing, Funding acquisition. **Jaana Oikkonen:** Conceptualization, Methodology, Writing – review & editing, Supervision. **Johanna Hynninen:** Conceptualization, Investigation, Writing – review & editing, Supervision, Funding acquisition.

#### Data availability

Raw DNA sequencing data is archived at the European Genome-phenome Archive (EGA) under study accession number EGAS00001006775.

## Declaration of Competing Interest

We have no conflicts of interest to disclose.

## Acknowledgement

This project received funding from the European Union's Horizon 2020 Research and Innovation Programme under Grant agreement No. 965193 (DECIDER), Sigrid Jusélius Foundation, Cancer Foundation Finland, and Sakari Alhpuuro foundation. The authors thank CSC – IT Center for Science for computational resources. The graphical abstract was created with BioRender.com.

## References

- R.L. Siegel, K.D. Miller, A. Jemal, Cancer statistics, 2019, *CA Cancer J. Clin.* 69 (1) (2019) 7–34, <https://doi.org/10.3322/CAAC.21551>.
- I. Ray-Coquard, P. Pautier, S. Pignata, et al., Olaparib plus bevacizumab as first-line maintenance in ovarian Cancer, *N. Engl. J. Med.* (2019) <https://doi.org/10.1056/nejmoa1911361> Published online.
- A. González-Martín, B. Pothuri, I. Vergote, et al., Niraparib in patients with newly diagnosed advanced ovarian Cancer, *N. Engl. J. Med.* (2019) <https://doi.org/10.1056/nejmoa1910962> Published online.
- K. Pennington, T. Walsh, M. Harrell, et al., Germline and somatic mutations in homologous recombination genes predict platinum response and improved overall survival in ovarian, fallopian tube, and peritoneal carcinomas, *Gynecol. Oncol.* 131 (1) (2013) 257–258, <https://doi.org/10.1016/j.ygyno.2013.07.028>.
- P.A. Konstantinopoulos, R. Ceccaldi, G.I. Shapiro, A.D. D'Andrea, Homologous recombination deficiency: exploiting the fundamental vulnerability of ovarian cancer, *Cancer Discov.* 5 (11) (2015) 1137–1154, <https://doi.org/10.1158/2159-8290.CD-15-0714>.
- R.E. Miller, A. Leary, C.L. Scott, et al., ESMO recommendations on predictive biomarker testing for homologous recombination deficiency and PARP inhibitor benefit in ovarian cancer, *Ann. Oncol.* 31 (12) (2020) 1606–1622, <https://doi.org/10.1016/j.annonc.2020.08.2102>.
- M. Moschetta, A. George, S.B. Kaye, S. Banerjee, BRCA somatic mutations and epigenetic BRCA modifications in serous ovarian cancer, *Ann. Oncol.* 27 (8) (2016) 1449–1455, <https://doi.org/10.1093/ANNONC/MDW142>.
- F. Perez-Villatoro, J. Oikonen, J. Casado, et al., Optimized detection of homologous recombination deficiency improves the prediction of clinical outcomes in cancer, *npj Precis. Oncol.* 6 (1) (2022) 1–13, <https://doi.org/10.1038/s41698-022-00339-8>.
- J.A. Ledermann, Y. Drew, R.S. Kristeleit, Homologous recombination deficiency and ovarian cancer, *Eur. J. Cancer* 60 (2016) 49–58, <https://doi.org/10.1016/j.ejca.2016.03.005>.
- J. Setton, J.S. Reis-Filho, S.N. Powell, Homologous recombination deficiency: how genomic signatures are generated, *Curr. Opin. Genet. Dev.* 66 (2021) 93–100, <https://doi.org/10.1016/j.cde.2021.01.002>.
- L.B. Alexandrov, J. Kim, N.J. Haradhvala, et al., The repertoire of mutational signatures in human cancer, *Nature*. 578 (2020) 94–101, <https://doi.org/10.1038/s41586-020-1943-3>.
- R.T. Hillman, G.B. Chisholm, K.H. Lu, P.A. Futreal, Genomic rearrangement signatures and clinical outcomes in high-grade serous ovarian Cancer, *JNCI* 110 (3) (2018) 265–272, <https://doi.org/10.1093/jnci/djx176>.
- D.C. Gulhan, J.J.K. Lee, G.E.M. Melloni, I. Cortés-Ciriano, P.J. Park, Detecting the mutational signature of homologous recombination deficiency in clinical samples, *Nat. Genet.* 51 (5) (2019) 912–919, <https://doi.org/10.1038/s41588-019-0390-2>.
- G. Macintyre, T.E. Goranova, D. De Silva, et al., Copy number signatures and mutational processes in ovarian carcinoma, *Nat. Genet.* 50 (2018) 1262–1270, <https://doi.org/10.1038/s41588-018-0179-8>.
- L.B. Alexandrov, et al., Signatures of mutational processes in human cancer, *Nature*. 500 (2013) 415–421, <https://doi.org/10.1038/nature12477>.
- P. Polak, J. Kim, L.Z. Braunstein, et al., A mutational signature reveals alterations underlying deficient homologous recombination repair in breast cancer, *Nat. Genet.* 49 (10) (2017) 1476–1486, <https://doi.org/10.1038/ng.3934>.
- E.A. Eisenhauer, P. Therasse, J. Bogaerts, et al., New response evaluation criteria in solid tumours: revised RECIST guideline (version 1.1), *Eur. J. Cancer* 45 (2) (2009) 228–247, <https://doi.org/10.1016/j.ejca.2008.10.026>.
- A. Cervera, V. Rantanen, K. Ovaska, et al., Anduril 2: upgraded large-scale data integration framework, *Bioinformatics*. 35 (19) (2019) 3815–3817, <https://doi.org/10.1093/bioinformatics/btz133>.
- A. Lahtinen, K. Lavikka, A. Virtanen, et al., Evolutionary states and trajectories characterized by distinct pathways stratify patients with ovarian high grade serous carcinoma, *Cancer Cell* 41 (2023) 1103–1117, <https://doi.org/10.1016/j.ccell.2023.04.017>.
- P. Van Loo, S.H. Nordgard, O.C. Lingjærde, et al., Allele-specific copy number analysis of tumors, *PNAS*. 107 (39) (2010) 16910–16915, <https://doi.org/10.1073/PNAS.1009843107>.
- J.G. Tate, S. Bamford, H.C. Jubb, et al., COSMIC: the catalogue of somatic mutations in Cancer, *Nucleic Acids Res.* 47 (2018) 941–947, <https://doi.org/10.1093/nar/gky1015>.
- S. Pikkusaari, M. Tumiati, A. Virtanen, et al., Functional homologous recombination assay on FFPE specimens of advanced high-grade serous ovarian cancer predicts clinical outcomes, *Clin. Cancer Res.* 29 (16) (2023) 3110–3123, <https://doi.org/10.1158/1078-0432.CCR-22-3156>.
- M.J. Landrum, J.M. Lee, M. Benson, et al., ClinVar: improving access to variant interpretations and supporting evidence, *Nucleic Acids Res.* 46 (D1) (2018) D1062–D1067, <https://doi.org/10.1093/NAR/GKX1153>.
- A. McKenna, M. Hanna, E. Banks, et al., The genome analysis toolkit: a MapReduce framework for analyzing next-generation DNA sequencing data, *Genome Res.* 20 (9) (2010) 1297–1303, <https://doi.org/10.1101/gr.107524.110>.
- D.I. Tommaso, M.P. Chatzou, E.W. Floden, P.P. Barja, E. Palumbo, C. Notredame, Nextflow enables reproducible computational workflows, *Nat. Biotechnol.* 35 (4) (2017) 316–319, <https://doi.org/10.1038/nbt.3820>.
- D.L. Cameron, J. Baber, C. Shale, et al., GRIDSS2: comprehensive characterisation of somatic structural variation using single breakend variants and structural variant phasing, *Genome Biol.* 22 (1) (2021) 1–25, <https://doi.org/10.1186/S13059-021-02423-X/FIGURES/5>.
- P. Priestley, J. Baber, M.P. Lolkema, et al., Pan-cancer whole-genome analyses of metastatic solid tumours, *Nature*. 575 (7781) (2019) 210–216, <https://doi.org/10.1038/s41586-019-1689-y>.
- G. Koh, A. Degasperi, X. Zou, S. Momen, S. Nik-Zainal, Mutational signatures: emerging concepts, caveats and clinical applications, *Nat. Rev. Cancer* 21 (10) (2021) 619–637, <https://doi.org/10.1038/s41568-021-00377-7>.
- E. Pleasance, A. Bohm, L.M. Williamson, et al., Whole-genome and transcriptome analysis enhances precision cancer treatment options, *Ann. Oncol.* 33 (9) (2022) 939–949, <https://doi.org/10.1016/j.annonc.2022.05.522>.
- S.Y.C. Yang, S. Lheureux, K. Karakasis, et al., Landscape of genomic alterations in high-grade serous ovarian cancer from exceptional long- and short-term survivors, *Genome Med.* 10 (1) (2018) 1–17, <https://doi.org/10.1186/S13073-018-0590-X/FIGURES/6>.
- A. Degasperi, X. Zou, T.D. Amarante, et al., Substitution mutational signatures in whole-genome-sequenced cancers in the UK population, *Science*. 376 (6591) (2022) <https://doi.org/10.1126/science.abc9283>.
- T. Masoodi, S. Siraj, A.K. Siraj, et al., Genetic heterogeneity and evolutionary history of high-grade ovarian carcinoma and matched distant metastases, *Br. J. Cancer* 122 (2020) 1219–1230, <https://doi.org/10.1038/s41416-020-0763-4>.
- A. McPherson, A. Roth, E. Laks, et al., Divergent modes of clonal spread and intraperitoneal mixing in high-grade serous ovarian cancer, *Nat. Genet.* 48 (2016) 758–767, <https://doi.org/10.1038/ng.3573>.
- A.-M. Patch, E.L. Christie, D. Etemadmoghadam, et al., Whole-genome characterization of chemoresistant ovarian cancer, *Nature*. 521 (2015) 489–494, <https://doi.org/10.1038/nature14410>.
- D.R. Hodgson, B.A. Dougherty, Z. Lai, et al., Candidate biomarkers of PARP inhibitor sensitivity in ovarian cancer beyond the BRCA genes, *Br. J. Cancer* 119 (11) (2018) 1401–1409, <https://doi.org/10.1038/S41416-018-0274-8>.
- A. Färkkilä, D.C. Gulhan, J. Casado, et al., Immunogenomic profiling determines responses to combined PARP and PD-1 inhibition in ovarian cancer, *Nat. Commun.* 11 (1) (2020) 1–13, <https://doi.org/10.1038/s41467-020-15315-8>.
- F. Batalini, D.C. Gulhan, V. Mao, et al., Mutational signature 3 detected from clinical panel sequencing is associated with responses to Olaparib in breast and ovarian cancers, *Clin. Cancer Res.* 28 (21) (2022) 4714–4723, <https://doi.org/10.1158/1078-0432.CCR-22-0749>.
- J.R. Tymon-Rosario, P. Manara, D.D. Manavella, et al., Homologous recombination deficiency (HRD) signature-3 in ovarian and uterine carcinosarcomas correlates with preclinical sensitivity to Olaparib, a poly (adenosine diphosphate [ADP]-ribose) polymerase (PARP) inhibitor, *Gynecol. Oncol.* 166 (1) (2022) 117–125, <https://doi.org/10.1016/j.ygyno.2022.05.005>.
- N. Shukla, M.F. Levine, G. Gundem, et al., Feasibility of whole genome and transcriptome profiling in pediatric and young adult cancers, *Nat. Commun.* 13 (1) (2022) 1–15, <https://doi.org/10.1038/s41467-022-30233-7>.
- E. Cuppen, O. Elemento, R. Rosenquist, et al., Implementation of whole-genome and transcriptome sequencing into clinical Cancer care, *JCO Precis Oncol.* (6) (2022) <https://doi.org/10.1200/PO.22.00245>.
- J.A. Dottino, H.A. Moss, K.H. Lu, A.A. Secord, L.J. Havrilesky, U.S. Food and Drug Administration–Approved Poly (ADP-Ribose) Polymerase Inhibitor Maintenance Therapy for Recurrent Ovarian Cancer, *Obstet. Gynecol.* 133 (4) (2019) 795–802, <https://doi.org/10.1097/AOG.0000000000003171>.
- For Patients, Foundation Medicine, Accessed November 6 <https://www.foundationmedicine.com/info/detail/for-patients> 2023.